Predicting damage in notched functionally graded materials plates through extended finite element method based on computational simulations

Hakim Siguerdjidjene
Materials, Processes and Environment (UR/MPE), Faculty of Technology, University M'hamed Bougara of Boumerdes, City Frantz Fanon, 35000 Boumerdes, Algeria
h.siguerdjine@univ-boumerdes.dz, http://orcid.org/0000-0003-1428-6786

Amin Houari
Laboratory of Motor Dynamics and Vibroacoustics (LDMV), Department of Mechanical Engineering, M'hamed Bougara University of Boumerdes, Boumerdes, Algeria
Department of Mechanical Engineering, LMSS, University of Djillali Liabes, Sidi Bel Abbes, Algeria
a.houari@univ-boumerdes.dz, http://orcid.org/0009-0004-2617-2182

Kouider Madani
Department of Mechanical Engineering, LMSS, University of Djillali Liabes, Sidi Bel Abbes, Algeria
koumad10@yahoo.fr, https://orcid.org/0000-0003-3277-1187

Salah Amroune
Mechanical Engineering Department, Faculty of Technology, University Mohamed Boudiaf of M'sila, Algeria
salah.amroune@univ-msila.dz, http://orcid.org/0000-0002-9565-1935

Mohamed Mokhtari
Department of Mechanical Engineering, RTF, National Polytechnic School of Oran, Algeria
mohamed.mokhtari@yahoo.fr, http://orcid.org/0000-0002-2014-1172

Barhm Mohamad
Department of Petroleum Technology, Koya Technical Institute, Erbil Polytechnic University, 44001 Erbil, Iraq
barhm.mohamad@epu.edu.iq, https://orcid.org/0000-0001-8107-6127

Chellil Ahmed
Laboratory of Motor Dynamics and Vibroacoustics (LDMV), Department of Mechanical Engineering, M'hamed Bougara University of Boumerdes, Boumerdes, Algeria
a.chellil@univ-boumerdes.dz, https://orcid.org/0000-0001-9467-4214

Abdelkrim Merah
Materials, Processes and Environment (UR/MPE), Faculty of Technology, University M'hamed Bougara of Boumerdes, City Frantz Fanon, 35000 Boumerdes, Algeria
LTSE, Faculty of Physics, USTHB, Bab Ezzouar 16111, Algiers, Algeria
abdelkrimerah@univ-boumerdes.dz, https://orcid.org/0000-0003-1376-5400

Raul D.S.G. Campilho
CIDEM, ISEP – School of Engineering, Polytechnic of Porto, Porto, Portugal
rds@isep.ipp.pt, https://orcid.org/0000-0003-4167-4434

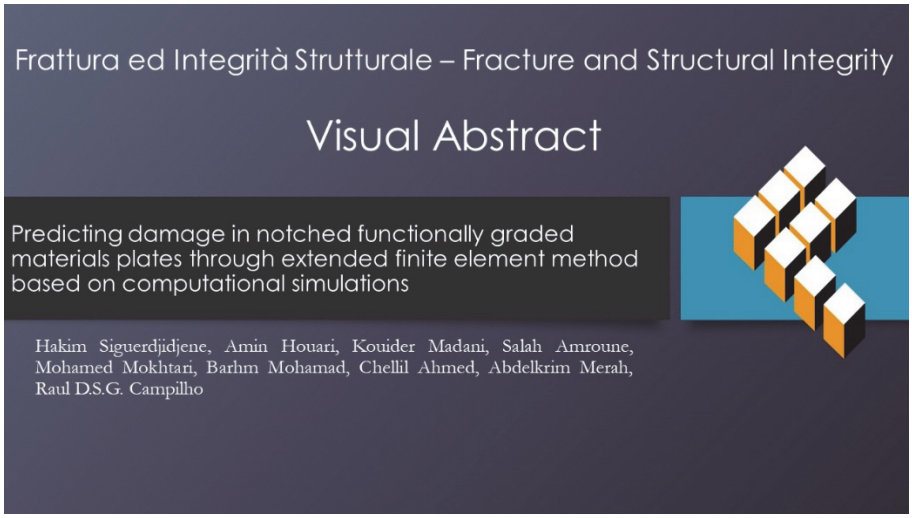

Citation: Siguerdjidjene, H., Houari, A., Madani, K., Amroune, S., Mokhtari, M., Mohamad, B., Ahmed, C., Merah, A., Campilho, R.D.S.C., Predicting damage in notched functionally graded materials plates through extended finite element method based on computational simulations, Frattura ed Integrità Strutturale, 70 (2024) 1-23.

Received: 19.04.2024
Accepted: 30.06.2024
Published: 03.07.2024
Issue: 10.2024

KEYWORDS. FGM (Functional Graded Materials), USDFLD (User-Defined Field Variables), XFEM (Extend Finite Element Method), Crack growth, Damage Prediction

INTRODUCTION

Due to their many advantages, functionally graded materials (FGMs) of the metal/ceramic type have known a wide use in various disciplines, in particular in high technology applications, justifying why their analysis currently presents a recent and important research axis. Their particularity compared to other materials is the change in their mechanical properties depending on the choice of the designer and without the presence of interfaces. In fact, these materials show a continuous property variation leading to structures with an optimized design in strength and functionality. The development of these materials (FGMs) has pushed their use in different fields such as nuclear reactors, medical and piezoelectric devices, and biological systems [1], due to their structural properties such as heat transfer, electrical conductivity, and others.

When a geometric discontinuity arises within the FGM material, the direction of material gradation is conditioned by the size and position of the notch. These geometric discontinuities are the main actor in the strength and mechanical behaviour of these structures. In fact, these constitute the areas of stress concentrations and the areas of crack initiation until total damage to the structure.

The stress concentration factor around a notch in a plate is studied by several researchers such as Shen et al. [2]. Recent numerical work by the isoparametric finite element method has been proposed by Kong et al. [3] and Gong et al. [4] to model structures in FGM. Other works, such as Wang et al. [5], have studied the effect of gradation on the stress concentration factor and have shown that this factor is completely different from that of a homogeneous material. Kubair et al. [6] also analysed, by the finite element method, a structure with a circular notch under a uniaxial load. On the other hand, the evaluation of the stress concentration around rectangular notches has been highlighted in the work of Dave and Sharma [7]. Graded structures according to different shapes of the notch have also been the objective of several researchers' efforts by the analysis of the stress concentration factor. Recently, Enab et al. [8] analysed the stress concentration in a structure with an elliptical notch while Cardenas-Garcia et al. [9] studied the variation of the radial and tangential thermal stresses and strains around a circular hole in an FGM structure. Yang et al. [10] also determined the stress concentration in

three dimensions of rectangular holes. Mohammadi et al. [11] used the Frobenius series solution to study the stress concentration factor around a circular notch under uniform biaxial stress.
In recent years, the XFEM technique has gained widespread popularity to analyse elastic, plastic, and fatigue crack propagation problems in conjunction with fracture mechanics and damage mechanics (Bansal et al. [12], Singh et al. [13] and Xu and Yuan[14]). In order to simulate the phenomenon of damage in FGM materials, several approaches have been proposed by researchers such as in the work of Asadpoure and Mohammad [15], Khazal et al.[16], Ueda [17], and Lee et al. [18], also by numerical methods [19-20] and experimentally [21, 22]. The use of the XFEM technique has many advantages in numerical computation, such as the elimination of remeshing and the introduction of enrichment functions in the structure. In addition, some researchers [23, 24] have applied the concept of FGM to study the mechanical behaviour of nanomaterials using a non-local model or a gradient elasticity model. Recently, Zivelonghi et al. [25] simulated the ductile fracture of an FGM structure based on CDM (continuum damage mechanics) and on its microstructure using the ABAQUS computer code. On the other hand, Gunes et al. [26] analysed the response impact under a reduced speed for FGM Al-SiC. An investigation was conducted to analyse the elastic-plastic behaviour of FGM material shells under various mechanical loadings by Huang et al. [27], Zhang et al. [28], and Jrad et al. [29]. By a gradation in the plane, Amirpour et al. [30] studied the model of damage in elastoplastic materials based on irreversible thermodynamics. The same analysis was carried out by Feulvarch et al. [31], on an FGM structure under buckling loading. Depending on the percentage and direction of gradation relative to the applied load, cracks in FGM materials behave in different ways. The initiation and evolution of a crack in FGM structures require a broad knowledge of the fracture behaviour. Actually, the crack in an FGM structure depends on several intrinsic or extrinsic parameters. All these parameters must be taken into account in the numerical simulation, where the crack trajectory is conditioned by the material gradation direction in FGM modelling. Jin et al. [32] have employed a cohesive zone model to examine the relationship between crack propagation and applied load for a Ti/TiB specimen. Khatri et al. [33, 34] analysed the growth of cracks in a notched isotropic plate using the XFEM technique. The authors examined the effect of the crack parameters and the notch radius. Hirshikesh et al. [35] also studied a field formulation for fracture in FGM materials. Another possible alternative is to locate the crack initiation using a damage-based approach. By these laws, one can model the degradation of the material and their critical zone [36]. Ritchie et al. [37] found that the initiation of a sudden rupture occurs when the value of the principal stress reaches its critical value. The maximum normal stress criterion was introduced by Erdogan and Sih [38]. It is based on the knowledge of the stress field at the crack tip. Another criterion such as the maximum energy restitution rate is proposed by Hussain et al. [39], showing that the crack propagates in the direction where the rate of restitution of the strain energy is maximum. In numerical predictions, the use of the USDFLD subroutine implemented in the ABAQUS code is one of the most efficient and frequently employed methods by many researchers, especially in FGM materials, such as Bouchikhi et al. [40], to determine the integral-J in a 2D structure of FGM type (TiB / Ti) and Mars et al. [41] for the analysis of the elastoplastic behaviour of FGM using user material subroutine (UMAT) and USDFLD. Martinez et al. [42] and Burlayenko et al. [43] investigated the crack propagation behaviour in FGM structures subjected to thermal shock conditions. Amirpour et al. [30] analysed damage in FGM structures with in-plane material properties variation using an elasto-plastic damage model.
A novelty of this work is the integration of a power law-based gradation in the FGM structure, where the thickness of the material plays a significant role. This approach allows for a more realistic representation of the FGM properties throughout the structure. Additionally, the combination of the Tamura-Tomota-Ozawa (TTO) model homogenization model for determining plasticity properties and the XFEM technique for crack initiation and propagation analysis provides a comprehensive understanding of the elastoplastic behaviour and damage progression in the FGM plate. The numerical linkage of FGM properties with the model geometry enhances the accuracy of the analysis and facilitates exploration of the effects of parameters such as the notch diameter and volume fraction exponent on crack localization and propagation. Validation of this numerical model reinforces the credibility and reliability of the obtained results.

GEOMETRIC MODEL OF THE FGM PLATE

A plate with central circular notch in FGM (Al/SiC) was considered, presented in the form of the set of surfaces (Fig.1a), of dimensions 125 mm in length, 25 mm in width, and 2 mm in thickness. The structure presents a central circular notch of variable radius from r=1.66 mm up to 5 mm with a pitch of 0.84 mm. Each surface exhibits mechanical properties as being a homogeneous and isotropic material.
The boundary conditions for the plate in tension are reproduced as follows (Fig. 1b): Embedding of the plate underside: $U_1=U_2=U_3=0$, $UR_1=UR_2=UR_3=0$ and uniaxial tensile stress of 250 MPa applied to the other side of the plate cross-section. The choice of this value is sufficient to induce damage in the FGM (Al/SiC) plate.

Tab. 1 provides the properties of the two constituents (Al/SiC) in the FGM material.
The finite element model is built with C3D8R elements, which present the best choice for the numerical modelling of the plate and are used in numerous examples of FGM modelling [29].

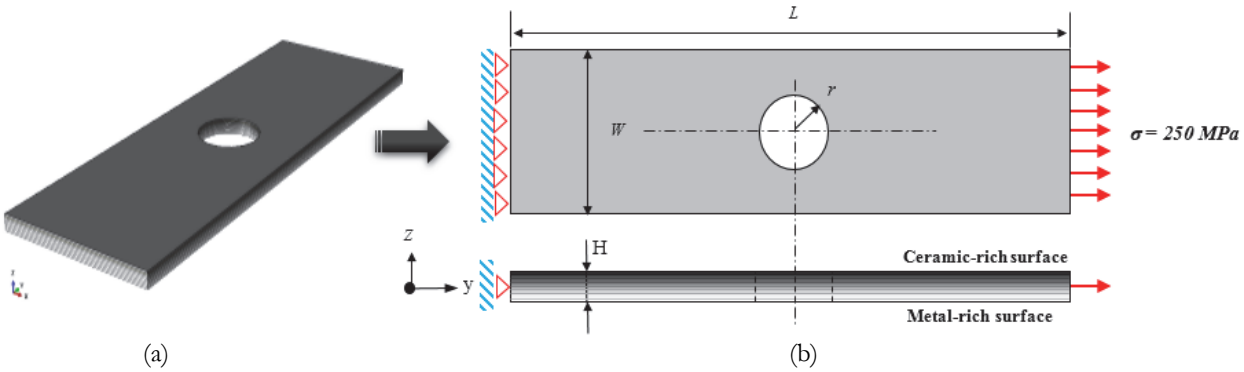

Figure 1: FGM structure modelled as a plate with a centrally located circular notch (Al/SiC) a) 3D, b) 2D

Property	Metal (Al)	Ceramic (SiC)
Young's Modulus E	67000 MPa	302000 MPa
Poisson's Ratio ν	0.33	0.17
Yield Stress σ_Y	95.1 MPa	-
Ultimate Stress σ_{UT}	160	1400
Fracture energy G_{Ic}	6.17 kJ/m²	0.065 kJ/m²
Tangent modulus H_p	1000 MPa	-
Ratio of stress to strain transfer "q"	4800 MPa*	

Table 1: Material properties of Aluminum alloy and SiC [44].

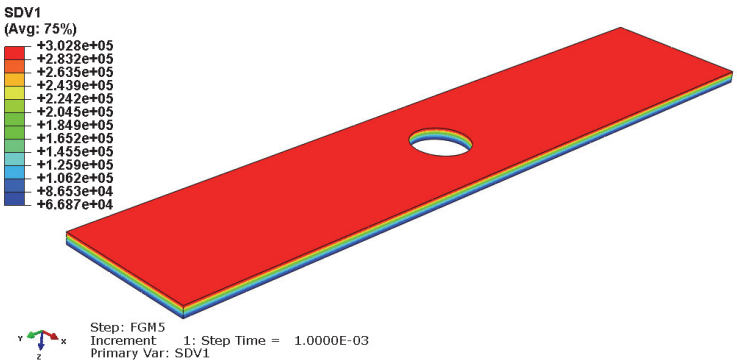

Figure 2: Linear distribution of Young's modulus (SDV1 of the unit MPa) through the thickness $h(z)$ of the plate with central circular notch in FGM (Al/SiC) via the USDFLD subroutine with power law.

GRADIENT OF FGM PROPERTIES

Traditionally, the properties of FGM are determined through experimental means. However, in ABAQUS, the graded mechanical properties of the FGM can be defined using a user subroutine, such as user material subroutine UMAT or USDFLD, which are called at the integration points. If a UMAT subroutine is utilized, the constitutive mechanical behaviour of the material must be programmed separately, making it impractical to use the pre-existing material models already available in ABAQUS. Consequently, the material gradient is incorporated by utilizing a user subroutine called USDFLD. This method allows the elastic properties of the material to be defined based on a field variable programmed

within the USDFLD subroutine. To ensure continuity of forces at the interfaces, a USDFLD subroutine is implemented in ABAQUS to specify the material properties of the FGM based on the coordinates of the integration points in the finite element model. In this particular study, integration points were systematically arranged throughout the thickness direction of the FGM plate, which consists of a metal/ceramic composite. The distribution of material properties across the thickness $H(z)$ of the FGM plate, according to a power law distribution, is shown in Fig. 2.

$$P(z) = (P_m - P_c).V_m + P_c \tag{1}$$

P represents the effective material property, $V_m = \left(\frac{z}{H} + \frac{1}{2}\right)^n$ is the metal volume fraction, n is the non-negative volume fraction exponent, and the subscripts c and m represent the ceramic and metal constituents, respectively.

Most existing studies on FGMs commonly employ the simple mixing rule to obtain effective material properties. Various functions such as power law (P-FGM), sigmoid (S-FGM), or exponential functions (E-FGM) are utilized to determine the volume fraction distribution function and equivalent material properties of FGMs. While the mixture laws are practical and straightforward, these do not provide information regarding the size, shape, and distribution of particles at the microstructural level. In the finite element method, the properties of the material are defined by the integration points through the USDFLD user subroutine. However, this method presents challenges in achieving exact solutions due to the unmanageable distribution of integration points. To address this limitation, this study proposes a technique based on a geometric model in which the distribution of material properties occurs at the surface level, with integration points located on the surfaces. By adopting this approach, the aim is to improve the element's performance in terms of the continuity of material property distribution and stress continuity at interfaces, thereby enabling accurate calculation of resulting stresses. This method seeks to obtain a volume fraction function that closely aligns with experimental observations using the finite element method. The FGM is developed without discontinuity (no layers to avoid residual stresses). So, geometrically the thickness of the plate in functional gradient materials can be formed by an assembly of an infinite number of surfaces (Fig.1a), in which each surface has its own mechanical properties. For this purpose, a surface method is proposed by subdividing the interval $\left[-\frac{H}{2}, \frac{H}{2}\right]$ of the plate:

$$z_i = -\frac{H}{2} + (i-1).e \tag{2}$$

where

z_i : coordinate of the surface relative to the global reference,

$i = 1, \ldots, m$: position of the surface in the FGM plate,

$e = \frac{H}{N}$: distance between two surfaces successively,

$m = N+1$: number of surfaces of the plate, and N: number of finite element layers.

To determine Eqn. (1), it is assumed that the surface is located exactly on the point of integration (Fig. 3). In addition, by the Simpson method, the point (i=1) is located exactly on the lower surface of the plate, and the type of Gauss integration, the point (i=1) is located near the lower surface [29]. So, the gradation of the FGM properties followed by the thickness is obtained by the points of the integrations:

$$h_g = \frac{e}{n_g} \tag{3}$$

where h_g is the distance between the two successive integration points, and n_g is the number of layers between integration points.

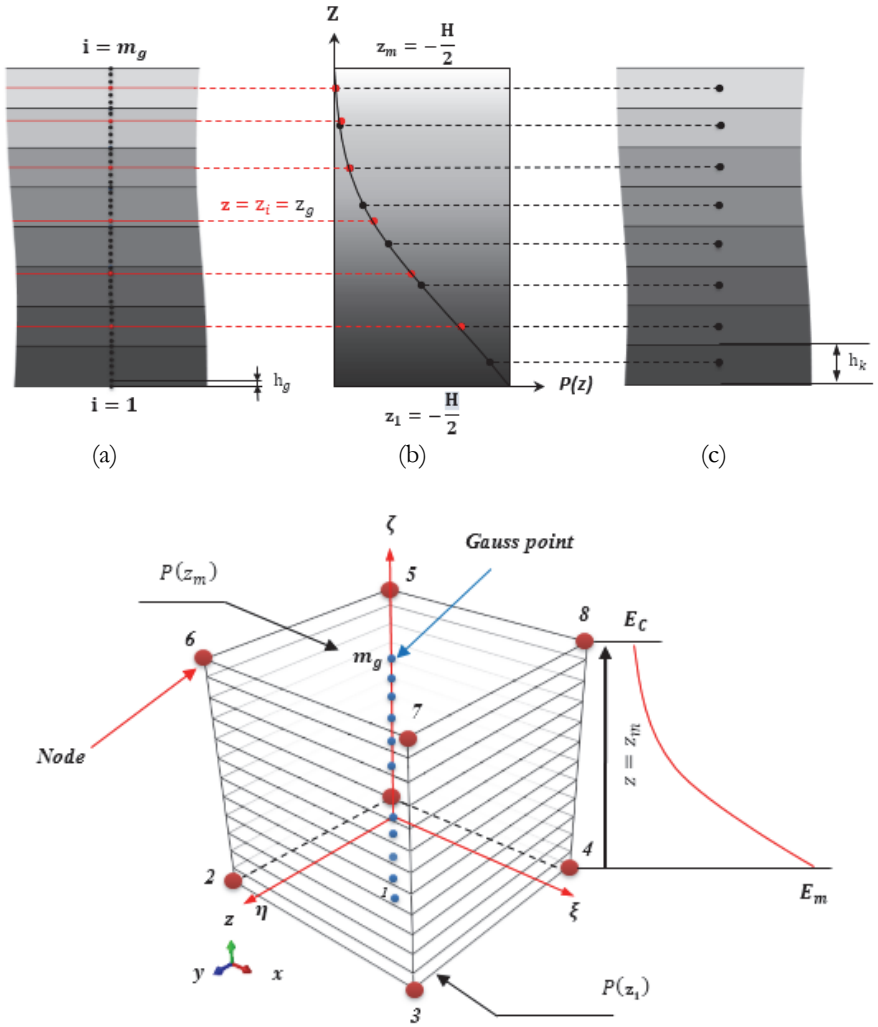

Figure 3: Reference geometry of the FGM and Gauss points. a) Graded surface b) Property variation along coordinate (z), c) homogeneous elements [45], d) The element SOLID-FGM and Gauss points.

So, Eqn. 1 becomes:

$$z_g = -\frac{e}{2} + (g-1)h_g \tag{4}$$

$$P(z_g) = \left[P(z_1) - P(z_m)\right]\left(\frac{z_g}{e} + \frac{1}{2}\right)^n + P(z_m) \tag{5}$$

where

$m_g = n_g + 1$ represents the total number of integration points within the interval H,

$g = 1, \ldots m_g + 1$ is the position number of integration point in the interval H,

h_g must be carefully chosen to minimize the error in the numerical results, especially when the number of integration points is minimal.

Where $P(z_g)$ denotes the effective material property of the FGM. Note that $P(z_1)$ and $P(z_m)$ are respectively the properties of the top and bottom faces of the interval H.

To obtain an accurate analysis of the FGM structure using C3D8R finite elements of the plate, the integration points through the thickness of the FGM plate are ordered continuously. As a result, multiple layers of elements are necessary in the finite element model to ensure an equal number of integration points throughout the thickness, as illustrated in Fig. 4.
In the elastoplastic behaviour of an FGM with a metal matrix reinforced with ceramic particles, isotropy and homogeneity are assumed for each surface. For this reason, the TTO model is used to determine the plastic properties of the FGM, which will be entered directly into ABAQUS.

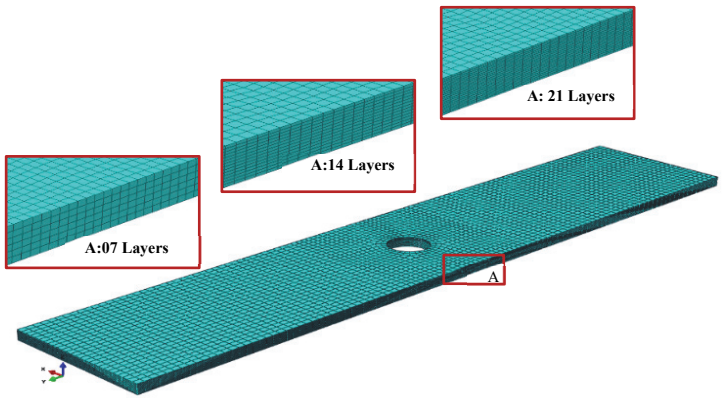

Figure 4: Description of the mesh density for an FGM plate according to thickness.

The TTO model is a metal alloy homogenization method and is used to evaluate locally effective elastoplastic parameters of the FGM (Al/SiC) compound. In the TTO model, the material mixture is treated as elastoplastic with linear isotropic hardening, for which the stresses and strains are related to the constitutive forces σ_m,σ_c, ε_m, ε_c [32, 46] by the relation:

$$\sigma = \sigma_m V_m + \sigma_c V_c \quad \text{and} \quad \varepsilon = \varepsilon_m V_m + \varepsilon_c V_c \tag{6}$$

In the TTO model, an additional parameter q is introduced, which represents the ratio of stress to strain transfer:

$$q = \left[(\sigma_c - \sigma_m) / (\varepsilon_c - \varepsilon_m) \right], \; 0 < q < \infty \tag{7}$$

The TTO model utilizes the elastoplastic properties of the metal constituent, which are determined by the modulus of elasticity E(z) of the FGM, the initial yield stress $\sigma_{Y_0}(z)$, and the tangent modulus $H_p(z)$. These properties are described by the following relationships:

$$E(z) = \left[\frac{q + E_c}{q + E_m} . E_m V_m + E_c . (1 - V_m) \right] / \left[\frac{q + E_c}{q + E_m} . V_m + (1 - V_m) \right] \tag{8}$$

$$H_p(z) = \left[\frac{q + E_c}{q + H_m} . H_m V_m + E_c . (1 - V_m) \right] / \left[\frac{q + E_c}{q + H_m} . V_m + (1 - V_m) \right] \tag{9}$$

$$\sigma_{Y_0}(z) = \sigma_{Y_{0m}} \left[\frac{q + E_m}{q + E_c} \frac{E_c}{E_m} . (1 - V_m) + V_m \right] \tag{10}$$

where $\sigma_{Y_{0m}}$ is the initial yield stress of metal, H_m is the tangent modulus of metal, $\varepsilon_{m_0} = \sigma_{Y_{0m}} / E_m$ and $\varepsilon_{Y_0}(z) = \sigma_{Y_0}(z) / E(z)$ are the initial yield strains of the metal and FGM Al/SiC. The Poisson's ratio $\nu(z)$ of the FGM just follows a rule of mixtures in the TTO model:

$$\nu(z) = \nu_m V_m + \nu_c V_c \tag{11}$$

XFEM IMPLANTATION FORMULATION FOR ELASTOPLASTIC ANALYSIS IN FGM

An analytical and numerical formulation was developed for the prediction of damage and crack propagation in FGM plates, especially in elastic-plastic behaviour [47]. The choice of the XFEM technique used in the calculations is based on several parameters, such as the damage criterion used, the gradation of properties in the structure (FGM), and crack propagation.

Governing equations

Let Ω be a three-dimensional domain of a continuous medium in two distinct parts, with boundary Γ, consisting of Γ_t and Γ, as shown in Fig.5. The boundary condition of displacement is imposed on Γ_u, the traction is applied on Γ_t and, given the presence of a cracked surface, the elastoplastic equilibrium equations with boundary conditions are written as follows [48].

$$\nabla\sigma + b = 0 \quad \text{in} \quad \Omega \tag{12}$$

$$\sigma.n \quad = \bar{t} \quad \text{in} \quad \Gamma_t \tag{13}$$

$$\sigma.n \quad = 0 \quad \text{in} \quad \Gamma_c \tag{14}$$

where n is the unit outward normal, σ is the Cauchy stress tensor, b is the body forces per unit volume, and $\bar{t}$ represents the traction vector. In the present investigation, small strains and displacements were considered.
The kinematics equations therefore consist of the strain–displacement relation:

$$\varepsilon = \varepsilon(u) = \nabla_s u \ \text{ and } u = \bar{u} \ \text{ on } \ \Gamma_u \tag{15}$$

where ∇s is the symmetric part of the gradient operator, u is the displacement field vector.

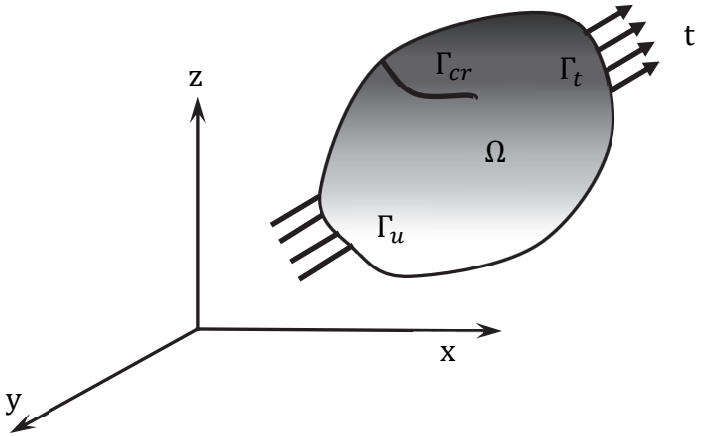

Figure 5: Schematic representation of homogeneous cracked body

Elastoplastic formulation

In the context of an FGM material consisting of a metal matrix reinforced by ceramic particles, it is assumed that each surface is both isotropic and homogeneous when exhibiting elastic-plastic behaviour. To model the elastoplastic behaviour of the FGM, the von Mises criterion and an isotropic hardening variable are employed. The rate expression for the stress-strain relationship of the elastoplastic material can be represented by the following equation:

$$d\sigma = C d\varepsilon^e = C\left(d\varepsilon - d\varepsilon^p\right) \tag{16}$$

where C is elastoplastic constitutive matrix of FGM. The change in strain is assumed to be divisible into elastic ($d\varepsilon^e$) and plastic components ($d\varepsilon^p$) for any increment of stress such that:

$$d\varepsilon = d\varepsilon^e + d\varepsilon^p \tag{17}$$

The strain tensor corresponds to the symmetric part of displacement gradient for an isoparametric element:

$$\varepsilon = \nabla_{sym}\boldsymbol{u} = Bu \tag{18}$$

where B is the strain-displacement matrix of shape function derivatives. The elastic component of increment strain can be written as:

$$d\varepsilon^e = [C]^{-1} d\sigma \tag{19}$$

where C is the constitutive matrix for three-dimensional linear elastic FGM. For the von Mises yield criteria, the yield surface can be described by:

$$f(\sigma, R) = \sigma_{eq} - \sigma_r = 0 \tag{20}$$

where $f(\sigma, R)$: is the yield function, and $\sigma_{eq} = \sqrt{\frac{3}{2}S.S}$: is the von Mises equivalent stress of FGM, where S is the deviatoric part of the Cauchy stress tensor:

$$S_{ij} = \sigma_{ij} - \frac{1}{3}\sigma_m \delta_{ij} \tag{21}$$

where σ_m is the mean stress, δ_{ij} is the Kronecker delta, and σ_r is the radius of the yield surface, defined by:

$$\sigma_r = \sigma_{Y0} + R(p) \tag{22}$$

where σ_{Y0} is the initial yield stress of the FGM, and $R(p) = H_P.p$ is the isotropic hardening (p is the internal variable corresponding to isotropic hardening and H_P is the hardening module). The rule of normality makes it possible to establish the following complementary relations:

$$d\varepsilon^p = d\lambda.N \quad \text{and} \quad N = \frac{\partial f}{\partial \sigma} = \frac{3}{2}\frac{S}{\sigma_{eq}} \tag{23}$$

where N: is the gradient of the yield function with respect to the stress tensor, and $d\varepsilon^p$: is the plastic strain rate. If the scalar (p), which is the accumulated plastic strain, is defined as the integration of the rate of the accumulated plastic strain during an iterative procedure.

$$p(t) = \int_0^t dp\, d\tau \tag{24}$$

where τ is an integration operator, and the rate itself is defined as:

$$dp = \sqrt{\frac{2}{3}d\varepsilon^p.d\varepsilon^p} \tag{25}$$

The scalar $d\lambda$ is the plastic multiplier, which is equal to the rate of the accumulated equivalent plastic strain. Given that $d\varepsilon^p$ represents the plastic strain rate, it can be demonstrated using Eqn. 23 and the von Mises equivalent stress σ_{eq}, that the plastic multiplier is equivalent to the rate of the accumulated plastic strain:

$$dp = \sqrt{\frac{2}{3}\left(\frac{3d\lambda}{2}\frac{S}{\sigma_{eq}}\right)\left(\frac{3d\lambda}{2}\frac{S}{\sigma_{eq}}\right)} = \sqrt{\frac{3}{2}d\lambda^2\frac{S}{\sigma_{eq}}\frac{S}{\sigma_{eq}}} \tag{26}$$

$$dp = d\lambda \tag{27}$$

The plastic multiplier $d\lambda$ in Eq. 22 is determined by using the consistency condition, to obtain the following expression:

$$\frac{\partial f}{\partial \sigma}d\sigma + \frac{\partial f}{\partial p}dp = \frac{\partial f}{\partial \sigma}d\sigma + \frac{\partial f}{\partial R}\frac{\partial R}{\partial p}dp = 0, \text{ and } \quad \dot{R} = \frac{\partial R}{\partial p}\dot{p} \tag{28}$$

Eq. 26 can be written as:

$$Nd\sigma - H_p d\lambda = 0 \quad \text{and} \quad H_p = \frac{dR}{dp} = \frac{d\sigma_{eq}}{d\varepsilon^p_{eq}} \tag{29}$$

Using Eq. 17 and Eq. 19 in Eq. 22 leads to:

$$d\varepsilon = [C]^{-1}d\sigma + d\lambda\frac{\partial f}{\partial \sigma} \tag{30}$$

After pre-multiplying both sides of Eq. 30 by $N^T C$:

$$N^T C\, d\varepsilon = N^T d\sigma + N^T C\, d\lambda N \tag{31}$$

$$N^T C\, d\varepsilon = H_p . d\varepsilon_{eq} + N^T C\, d\lambda N \tag{32}$$

The following expression is obtained for the plastic multiplier:

$$d\lambda = d\varepsilon^p_{eq} = \frac{N : C.d\varepsilon}{N : C : N + H_P} \tag{33}$$

Finally, by substituting the expression of the plastic part $d\varepsilon^p = d\lambda.N$ into Eq. 17, the elastoplastic tangent modulus is derived as:

$$C^{ep} = C - \frac{(N : C)\otimes(N : C)}{N : C : N + H_P} \tag{34}$$

At last, the updated stresses (σ) at the conclusion of the time step (Δt) can be expressed as follows:

$$\sigma_{n+1} = \sigma_n + d\sigma \tag{35}$$

The subscript (n+1) indicates the values corresponding to the end of the time increment.

3D XFEM formulation for FGM

The enrichment functions in the XFEM technique require a high number of integration points to obtain satisfactory results. The XFEM technique is implemented in the ABAQUS code [49] and is not compatible with user-defined finite elements in graded materials (FGM). Indeed, for the XFEM technique to be implemented by the user it is necessary to use a USDFLD subroutine in the ABAQUS code to simulate the force equilibrium with linear finite elements in three dimensions. The weak form of the governing equation for a solid mechanics problem can be expressed as:

$$\int_{\Omega} \varepsilon(u) : C : \varepsilon(u) d\Omega = \int_{\Omega} b.u d\Omega - \int_{\Gamma} \overline{t}.u d\Gamma \tag{36}$$

The above equation can be written in the form of the finite element procedure, as [12]:

$$\int_{\Omega} B^T \sigma d\Omega = \int_{\Omega} N_i^T b d\Omega - \int_{\Gamma} N_i^T \overline{t}.d\Omega \tag{37}$$

By substituting the trial and test functions from Eqn. (36) into Eqn. (37) and leveraging the flexibility of nodal variations, the ensuing discrete system of linear equations is attained:

$$\left\{ \mathrm{f}^{\mathrm{e}} \right\} = \left[k^e \right] \left\{ \mathrm{u}^b \right\} \tag{38}$$

The element stiffness matrix, denoted as k^e, and the external load vector, denoted as f^{e}, are provided as follows:

$$\mathrm{f}^{\mathrm{e}} = \left\{ \mathrm{f}_i^u \quad \mathrm{f}_i^a \quad \mathrm{f}_i^{b1} \quad \mathrm{f}_i^{b2} \quad \mathrm{f}_i^{b3} \quad \mathrm{f}_i^{b4} \right\} \tag{39}$$

$$\left[k^e \right] = \left[\mathrm{k}_{ij}^{\theta\beta} \right] = \int_{\Omega^{\mathrm{e}}} \left(\mathrm{B}_i^{\theta} \right)^T [\mathrm{C}] \mathrm{B}_j^{\beta} \mathrm{d}\Omega \quad \textit{and} \quad \theta, \beta = u, a, b \tag{40}$$

$$\mathrm{f}_i^u = \int_{\Omega} N_i b d\Omega + \int_{\Gamma} N_i \overline{t} d\Gamma \tag{41}$$

$$\mathrm{f}_i^a = \int_{\Omega} N_i \left(\mathrm{H}_f(\mathrm{x}) - \mathrm{H}_f(\mathrm{x}_i) \right) b d\Omega + \int_{\Gamma} N_i \left(\mathrm{H}_f(\mathrm{x}) - \mathrm{H}_f(\mathrm{x}_i) \right) \overline{t} d\Gamma \tag{42}$$

$$\mathrm{f}_{\mathrm{i}}^{\mathrm{b}\alpha} = \int_{\Omega} \mathrm{N}_{\mathrm{i}} \left(\mathrm{F}_{\mathrm{j}}(\mathrm{x}) \right) \mathrm{b} \mathrm{d}\Omega + \int_{\Gamma} \mathrm{N}_{\mathrm{i}} \left(\mathrm{F}_{\mathrm{j}}(\mathrm{x}) \right) \overline{\mathrm{t}} \mathrm{d}\Gamma \quad (\alpha = 1 - 4) \tag{43}$$

In which t is the external force, b is the body force, C is the elasticity matrix, N_{i} are standard shape functions, and B_i^{θ} and B_j^{β} are the matrix of shape function derivatives. In numerical predictions of the three-dimensional crack behavior by the XFEM technique, the elastoplastic behavior is given by Eqn. (44), and the displacement field variable u(x) for a domain that includes a crack is represented as follows [50]:

$$\mathrm{u}^b(\mathrm{x}) = \sum_{\mathrm{i}=\mathrm{M}} \mathrm{N}_{\mathrm{i}}(\mathrm{x}) \mathrm{u}_{\mathrm{i}} + \sum_{\mathrm{i} \in \mathrm{N}_{\mathrm{d}}} \mathrm{N}_{\mathrm{i}}(\mathrm{x}) \mathrm{H}_f(\mathrm{x}) \mathrm{a}_{\mathrm{i}} + \sum_{\mathrm{i} \in \mathrm{N}_{\mathrm{p}}} \mathrm{N}_{\mathrm{i}}(\mathrm{x}) \left(\sum_{\mathrm{j}=1}^{4} \mathrm{F}_{\mathrm{j}}(\mathrm{x}) \mathrm{b}_{\mathrm{i}}^{\mathrm{j}} \right) \tag{44}$$

In the given context, M represents the set of nodes within the mesh, and u_{i} represents the classical degree of freedom at node i. $\mathrm{N}_{\mathrm{i}}(\mathrm{x})$ refers to the classical finite element shape functions associated with node i. Additionally, a and b are supplementary degrees of freedom introduced to the common degrees of freedom. $\mathrm{H}_f(\mathrm{x})$ denotes the Heaviside function, and $\mathrm{F}_{\mathrm{j}}(\mathrm{x})$ represents a specific set of four tip enrichment functions, as outlined in reference [48]:

$$\left\{F_j(x)\right\}=\left\{r^{\alpha}\sin\frac{\phi}{2},r^{\alpha}\cos\frac{\phi}{2},r^{\alpha}\sin\frac{\phi}{2}\sin\frac{\phi}{2},r^{\alpha}\cos\frac{\phi}{2}\sin\frac{\phi}{2}\right\} \tag{45}$$

Where (r,ϕ) are the polar coordinates in the local axes at the crack tip. For the linear analysis, the value of exponent $\alpha = 0.5$ was used. For the nonlinear analysis, the value of exponent $\alpha = 1/(1+\eta)$ was considered instead, where η is the strain hardening exponent that depends on the FGM. The introduction of FGM properties using the TTO model based on the metal stress-strain curve is determined by means of the Ramberg-Osgood equation from the offset yield strength values (Fig.6).

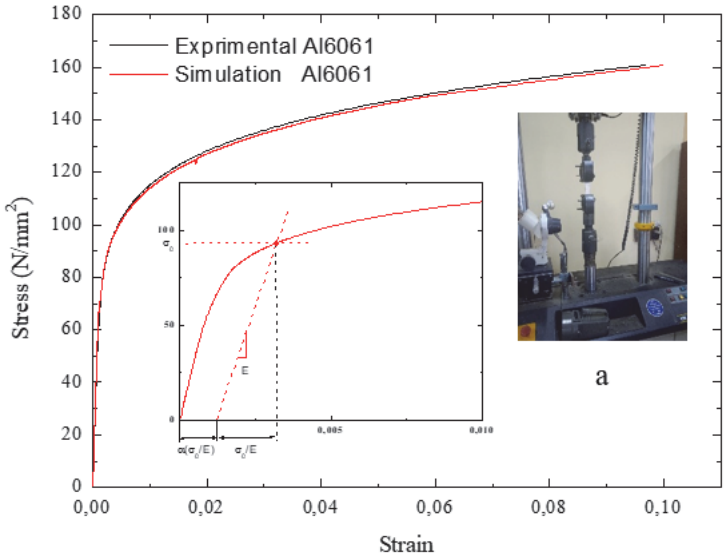

Figure 6: Representation and comparison of the Al6061 experimental and numerical stress-strain curves by the Ramberg-Osgood equation

DAMAGE FGM

For the damage behaviour in the present analysis, a non-local damage mechanics approach was used, which requires the mesh regularization chosen in this work. The maximum principal stress criterion MAXPS is used to promote crack initiation as well as its propagation direction. The choice of Maximum stresses as the criterion for damage initiation is used to reduce the sensitivity of the mesh in non-local approaches (Continuum damage mechanics). Any Gaussian point exceeding the critical value 1 of the damage parameter f should be examined [47].

$$f=\frac{\sigma_{eq}}{\sigma_{UTS}}=1 \quad \text{with} \quad \sigma_{UTS}=\sigma_{UTSm}.\left[\frac{q+H_m}{q+E_c}\frac{E_c}{H_m}.(1-V_m)+V_m\right] \tag{46}$$

where σ_{eq} is the equivalent von-Mises stress of FGM, σ_{UTS} is the ultimate tensile strength of FGM, σ_{UTSm} is the ultimate tensile strength of metal, $f=1$ means the occurrence of damage within an enriched element, and H_m is the tangent modulus of the metal. The FGM properties were introduced directly into the ABAQUS calculation code using the MATLAB-assisted gradient surface technique.

For the damage evolution, the energy approach [51] based on the critical strain energy release rate (G_{IC}) is used to model the crack propagation.

$$G=\int_0^{u^p}\sigma du^p \quad \text{where} \quad G=\int_{\bar{\varepsilon}_0^p}^{\bar{\varepsilon}_f^p}L\sigma d\bar{\varepsilon}^p \tag{47}$$

where $\bar{u}^p = L.d\bar{\varepsilon}^p$ is the equivalent plastic displacement and σ is the stress, L is the length of the element, $\bar{\varepsilon}_0^p$, $\bar{\varepsilon}_f^p$ are respectively the initial and final graduated plastic strains and G_f^C is the critical energy release rate of FGM. G_f^C can be expressed by a mixing rule as follows [52]:

$$G_f^F = G_f^m V_m + G_f^c V_c \tag{48}$$

G_f^m , G_f^c are the critical energy release rates of the metal and ceramic, respectively. At the same time, the energetic approach defines the opening of a crack of length L in a material. This approach is available in the ABAQUS calculation code with two types, namely linear damage variation as a function of absorbed energy or displacement, and exponential damage variation. In the stiffness degradation for the linear process, the calculation of the D parameter increment is based on the following Eqn. (49).

$$D = \frac{\int_0^{\bar{\varepsilon}_f^p} L\sigma d\bar{\varepsilon}^p}{G_f^F} \tag{49}$$

In the numerical calculation, the damage evolution in a zone of the structure depends on the field of Gauss points around crack front. When solving the crack propagation, the stress value at the Gauss points near the crack front is very high due to the singularity. Since the crack initiation is based on the graded critical stress in the structure, its propagation is done from one Gauss point to the next depending on the location of each and its introduced critical values. Therefore, the crack also develops when a small region near the crack front is totally damaged. The characteristic length works well with the damage evolution criterion introduced in the form of energy, and it is also noted that the mesh size in the crack propagation zone is chosen to determine its propagation curve. These element sizes remain the same for other geometries and loading conditions, but vary according to the material conditions.

IMPLEMENTATION OF THE MODEL

The behaviour model was implemented in a standard ABAQUS finite element code via the USDFLD subroutine using MATLAB for a variation of the material properties with thickness by a function of the variable field. The geometry is linked to the USDFLD program generated by ABAQUS.CAE and is presented in an ABAQUS.INP file (Fig. 7), which are used in the calculation by a coupled approach with the USDFLD.for file. This procedure is programmed in subroutine in an independent file (see appendix).

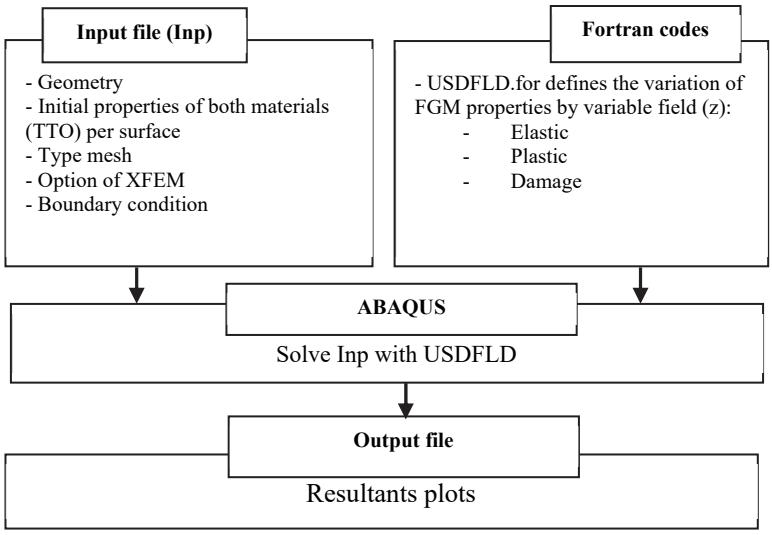

Figure 7: Implementation of the FGM model in standard ABAQUS

EXPERIMENTAL VALIDATION OF A NUMERICAL MODEL

To validate the proposed numerical approach, the experimental results of Surya and Prasanthi [53] on FGM (Al/SiC) (Fig.8) were used, to have a reliable comparison all depends on the choice of the appropriate mesh. Actually, the sensitivity of the mesh in this proposed technique is related to the introduction of experimental properties per surface and in the sense of the number of integration points. These integration points are a function of the number of elements along the gradation direction of the present analysed FGM structure. The gradation between the surfaces (Gauss points) where the experimental properties are introduced is done by a purely geometrical approach, and is conditioned by shape functions that replace the volume fraction in the gradation direction.

Another important parameter that was the subject of the sensitivity analysis is the number of surfaces introduced and the number of Gauss points between these surfaces. The type of C3D8R element chosen has no influence on how the gradation is approached geometrically, but it does play a crucial role in the interpolation of the stress-strain field and in damage behaviour, such as crack initiation and propagation. The mesh element C3D8R showed predictions closer to the experimental results. Similarly, this type of element is appropriate with the damage evolution criterion used in this analysis and is known to have advantages with the use of XFEM.

After several mesh sensitivity tests on the model, it was concluded that the C3D8R element type with more Gauss points (mesh density) and their location facilitate the advancement of the crack and easily allow the correct evolution of the damage variable.

In order to validate our numerical model, we tried to integrate the mechanical properties from the experimental, and which are really rare, and found in the literature [53] for an FGM structure with a material gradation according to its thickness and stressed in uniaxial tension along its length so as to validate our subroutine where we have integrated the different equations proposed for modeling the damage of the FGM.

Fig. 8 presents a validation of the proposed approach with the experimental results. a good agreement is noted between the traction curve for the proposed numerical model and the experimental traction curve. the curves following the same pace even in elastoplastic behavior of the structure and until total damage. A difference is noted in relation to the point of maximum stress or a slight difference is noted, all depending on the mesh density and the number of surfaces proposed for material gradation.

We clearly notice that with more surfaces to introduce the material properties of the FGM, the numerical predictions are closer to the experimental ones than those which have less surface (integration Gauss points), but with more layers. This clearly explains an appropriate optimum choice between these two parameters.

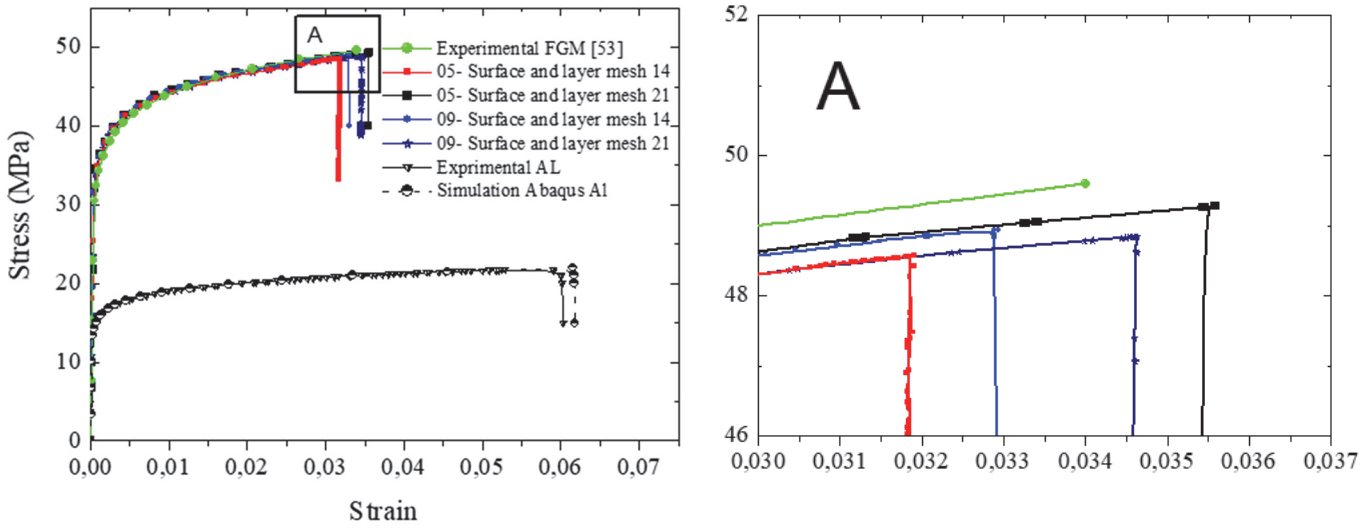

Figure 8: Validation of the element density of the FGM (Al/SiC) numerical model with the experimental curve [53].

RESULTS AND ANALYSIS OF DAMAGE

The analysis with the gradation of the mechanical properties according to the thickness aims at validating the gradation approach by considering the damage of the structure in FGM. The major advantage of this approach is to avoid any discontinuity in the distribution of stress or strain in the structure and to simplify the study of the elastic-plastic behaviour coupled with the damage criterion. The proposed numerical technique concerning the geometrical grading approach shows its effectiveness in the results considering different parameters to be evaluated.

Effect of notch size and FGM volume fraction

In this part of the study, and after the positive validation with the experimental results and the mesh sensitivity, force-displacement curves are shown, since it is important to present not only the response of the structure until its damage but also the behaviour of the crack under the various parameters, from its initiation through its path of propagation to its critical length that causes the global damage to the structure. The location of the notch with these different dimensions will allow to cause not only plasticization but also crack initiation until the failure. It is also important to specify that, at the level of these notches, plasticization remains important and occurs with the appearance of a bending moment as the load increases. This is simply due to the direction of the gradation (ductile/fragile) of the FGM, which is according to the thickness of the analysed structure.

The following figures present the results of an FGM structure graded by 14 introduced surfaces. These present both the response under the effect of the notch radius and the exponent of the volume fraction. However, one can see an inter-dependence of the effect of these two parameters, which will be able to present a good correlation in order to identify the damage of the FGM plate.

Fig. 9 presents the load-displacement response and crack length evolution of the analysed structure in FGM (Al/SiC) for a gradation exponent n=0.5. It can be clearly seen that the plasticity behaviour increases rapidly with the reduction of the notch radius from 1.66 mm to 5 mm.

The mentioned plasticity is one of the reasons why the strength of the plate increases. Indeed, the latter is increased by stress absorption on one side and crack propagation blocking after initiation on the other side, as in the case of notch radius r=1.66 mm. However, the response of the structure up to crack initiation is conditioned by the value of the notch radius. Once the crack takes its way into the structure, other parameters condition the strength of the plate, such as the symmetry of the structure and the gradation according to the thickness for the exponent n=0.5. The large length of crack propagation is caused by very small displacements for large notch radii. For minimum notch radii relative to the width of the plate, the resistance to the applied load is considerable, so that once the crack is initiated in the plate at the notch its propagation towards the free edge of the plate requires more energy than for the case of cracks which initiate at the level of large notch.

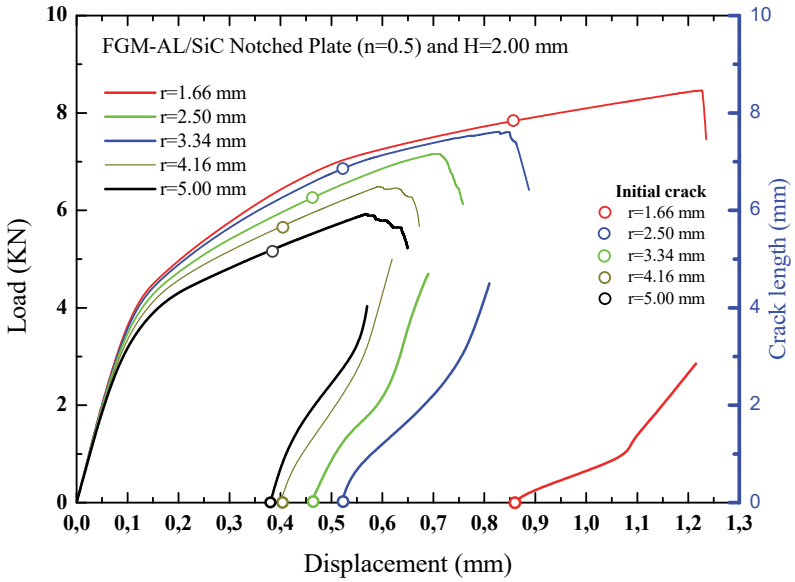

Figure 9: Load-displacement response and crack length of FGM (Al/SiC) for n=0.5.

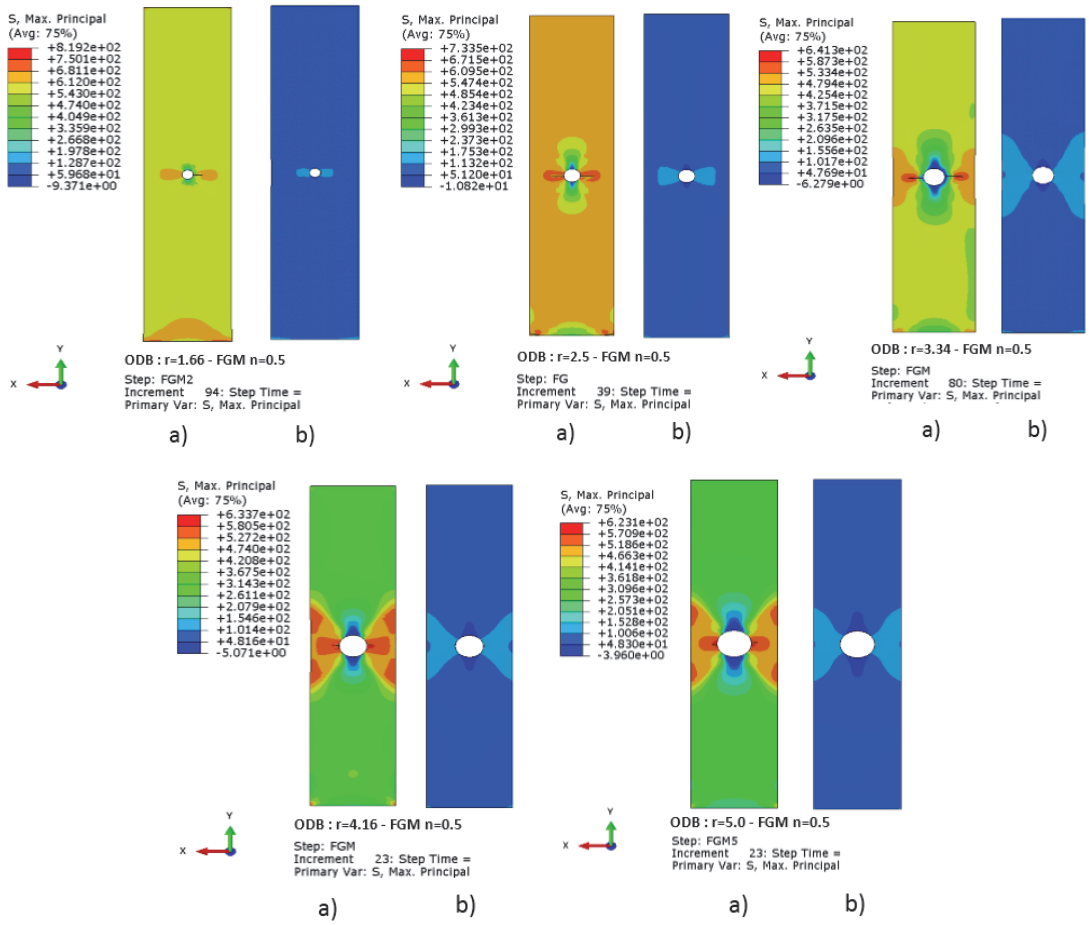

Figure 10: Critical crack length with the normal stress level in the FGM (Al/SiC) plate for n=0.5 and different notch sizes; a) Ceramic-rich surface, b) Metal-rich surface

Fig. 10 presents the variation of the critical length for each structure according to the dimension of the notch under an exponent of gradation equal to 0.5 of an FGM material graded according to the thickness of the structure. It can be seen that the stresses present an almost symmetrical distribution around the notch with respect to the SiC side due to the presence of cracks, while the aluminium side remains uninitiated. At different levels of stress, the cracks reach their critical length in relation to the ceramic side to be able to propagate gradually towards the aluminium side. This critical length of the crack depends on the dimensions of the notch.

Fig. 11 shows the force-displacement curve as a function of the value of the notch radius of the FGM plate under the effect of an exponent of a volume fraction n=1. It is clearly noted that the effect of stiffness is introduced by the gradation under an exponent of n=1. In fact, the FGM-Al/SiC structure displays in its response more loading but less deformation capacity, which makes the structure stiffer. The critical length from which the structure is totally damaged grows progressively and simultaneously with the increase of the notch radius, and also with the value of the gradation exponent. The amount of load expended to advance the crack becomes inversely proportional with the reduction of the notch radius.

Fig. 12 presents the level of Max stress in the FGM structure under a gradation exponent of n=1. It is clearly noted that the crack reaches a variable critical length for different diameters of the notch. Moreover, at the level of the most brittle side, the crack starts quickly with a rather significant propagation. It is also noticed that the crack can develop on one side as well as on both sides of the notch, and that each structure, depending on the dimension of its notch is solicited differently (value of the normal constraint is different), which thereafter involves the initiation of the crack with its own critical length from which the global damage of the structure is produced.

Fig. 13 simultaneously presents, for a value of the gradation exponent n=2, the effect of the dimensions of the notch on the elastic-plastic behaviour until the damage of the structure in FGM and the behaviour of the crack from its initiation to its critical length taking into account the amount of load to be spent by its advancement.

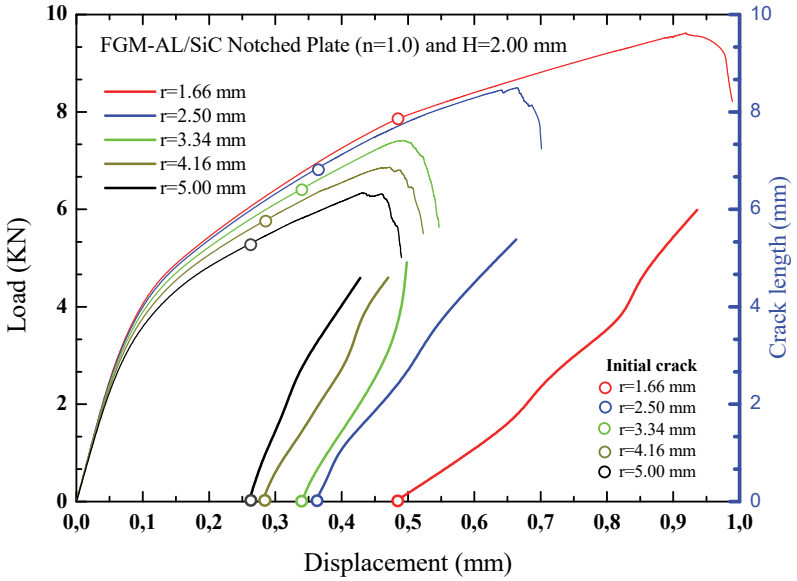

Figure 11: Load-displacement response and crack length of FGM (Al/SiC) for the exponent fraction n=1.0.

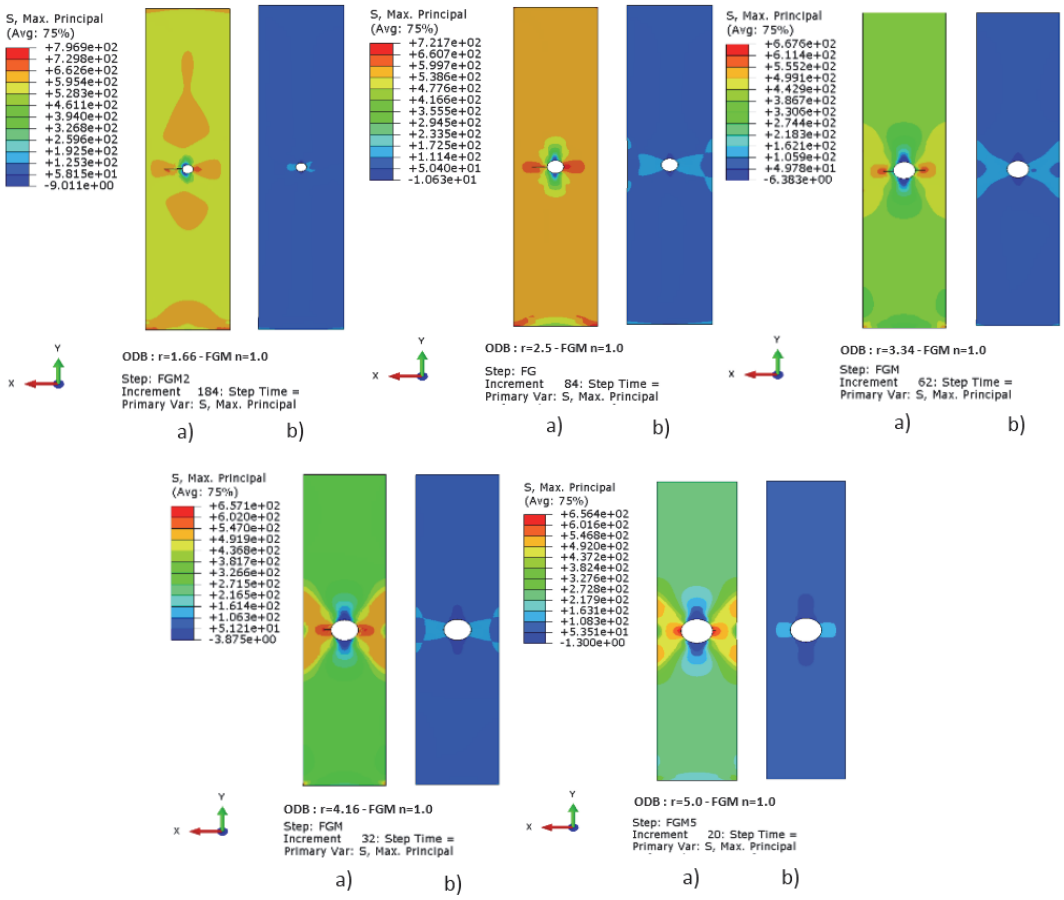

Figure 12: Critical crack length with stress field of an FGM (Al/SiC) plate for n=1 and different notch diameters; a) Ceramic-rich surface, b) Metal-rich surface

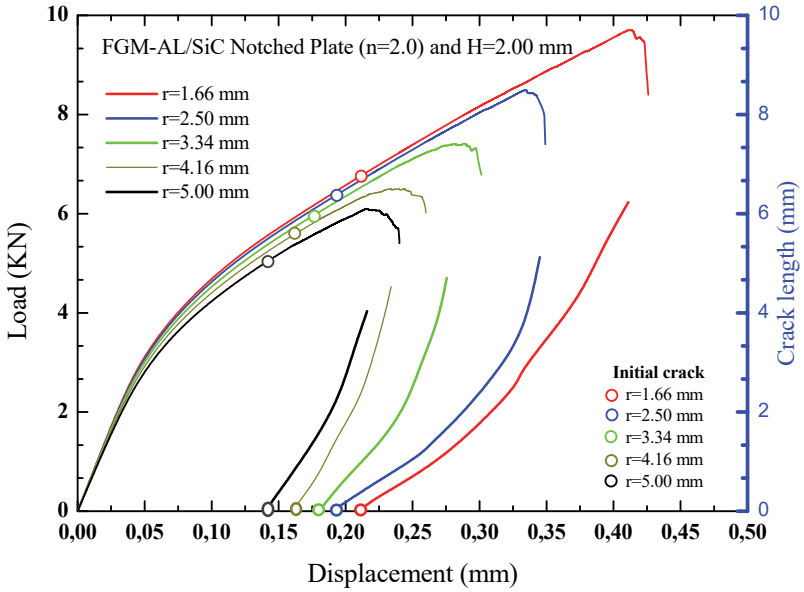

Figure 13: Load-displacement response and crack length of FGM by n=2.0

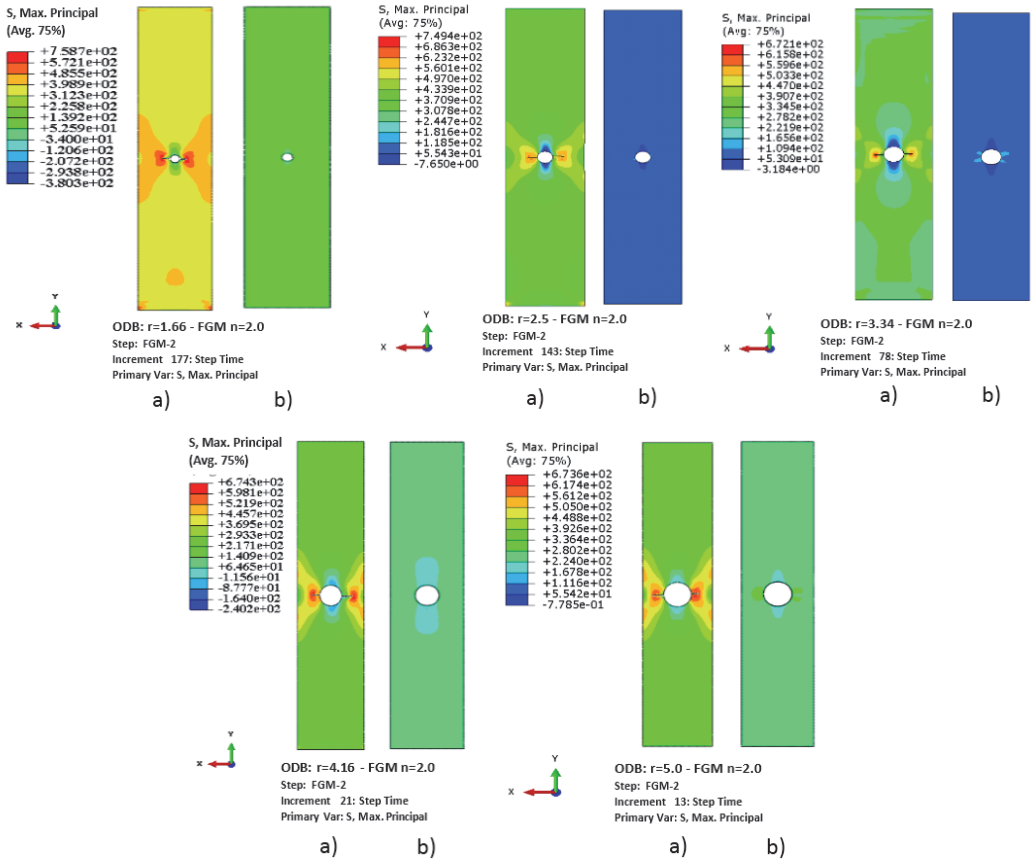

Figure 14: Critical crack length with stress field of an FGM Al/SiC plate for n=2 and different notch diameters a) ceramic rich side, b) metal rich side

It is clearly noticeable that the structure is quickly damaged when the dimension of the notch is important but in a different way under the effect of the value of the exponent n. Indeed, the more the structure is fragile in gradation, the more the damage occurs at higher forces and lower displacements. This behaviour can be explained by the appearance of the plastic part of the three previous results. It can also be found that, the smaller the notch size, the greater the critical crack length

that corresponds to the total damage of the structure, except for the brittle structures in gradation, which presents an important advancement of the crack at too low displacements.
Fig. 14 shows crack propagation as soon as it reaches its critical length for different diameters of the notch and under an exponent of gradation n=2. It is clear that, for both cases, between the aluminium side and the SiC side, the crack appears and reaches its critical length in the SiC side, while the other side is still uninitiated by the crack. Each structure, depending on the size of its notch, has its own critical length of the crack from which the global damage of the structure is produced.

Failure load under effect of dimension of notch and exponent faction

It is important to analyse the effects of the different parameters undertaken in this study, namely the diameter of the notch and the gradation exponent of the FGM material on the resistance of the plate and more precisely the initiation of damage, and to try to find a correlation between these two parameters in order to better identify their simultaneous influence on the resistance of our structure. Indeed, the presence of geometric discontinuity can reduce the strength of the structure to 35%, as shown in Fig. 15.

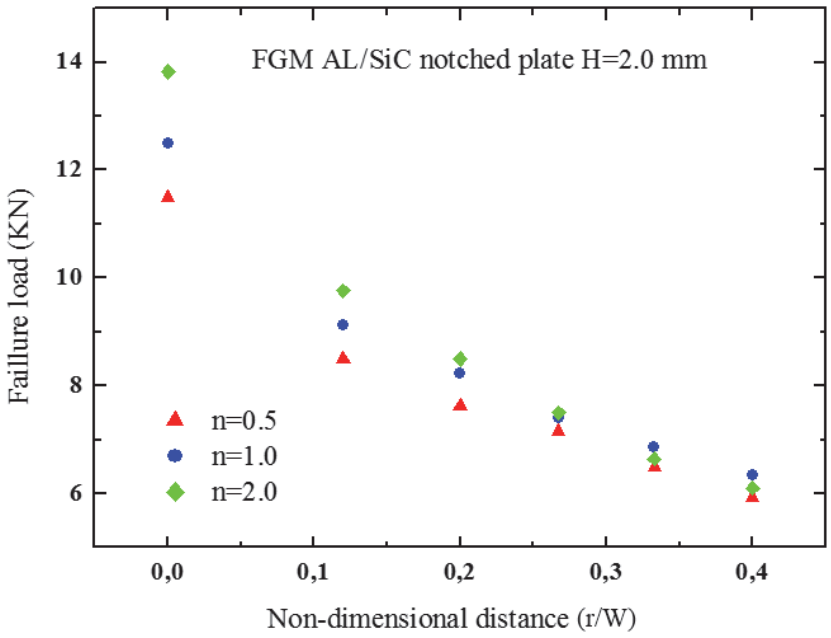

Figure 15: Failure load under effect of dimension of notch and exponent fraction.

Fig. 15 shows the effect of the notch size and the gradation exponent "n" on the damage strength. If the notch size is large, the structure shows a smaller strength for any gradation of the structure in FGM. The strength also diminishes if the gradation exponent decreases. However, if the diameter of the notch is small, the effect of the exponent of the volume fraction clearly appears on the value of the damage force. On the other hand, if the diameter of the notch is large, the effect of the exponent of the volume fraction disappears, which means that the concentration of the stress in the presence of the notch imposes itself on the value of the damage force more than the effect of the gradation exponent.

CONCLUSION

The methodology proposed in this study, which incorporates precise characterization of material properties in the thickness direction, has convincingly showcased its effectiveness in accurately predicting the elastic-plastic behaviour and subsequent damage of the FGM structure across various notch dimensions. The numerical findings obtained from this research yield the following noteworthy observations:

- The accuracy of the results of the proposed technique is based on the gradation of the two materials on a purely geometric model related also on the quality of the mesh in terms of element density.
- By dividing the structure into several surfaces, it is easy to introduce the mechanical properties of the two substrates according to the law of mixing as a function of thickness, which facilitates the choice of conditioning the gradation

according to the actual development of the FGM. The geometrical approach ensures the continuity of this gradation between its surfaces and thereafter to get much closer to a gradation similar to that of the experimental case.
- The interval between selected gradation surfaces as well as the density of elements are the parameters that ensure the accuracy of the results for validation with the experimental results in elastic-plastic behaviour until damage.
- The predictive capabilities of the modelling using the geometric approach technique allowed to evaluate some parameters that condition the response of the notched structure in FGM until its damage.
- Thanks to the XFEM separation technique, which is appropriate with the damage criterion and the geometric grading approach used, it was possible to induce continuous damage progression in the FGM structure.
- The initiation and the critical length of the crack are well conditioned by the dimension of the notch in our FGM structure.
- The amount of load expended per advanced crack length in FGM materials is a function of the notch size in the FGM material.
- In all cases, damage to FGM plates occurs at the notch, around which the structure becomes weakened, but at loading and crack propagation path levels depending on the notch size and volume fraction exponent,

Following the conclusions drawn above, and by using the new geometric gradation approach in FGM structures, this work has provided new modelling that remains exploitable for more problems, such as predictions of crack propagation path and their velocity, as well as damage in elastic-plastic behaviour for any geometric shape of the structure and along any gradation direction, and thus it opens interesting directions for further research.

REFERENCES

[1] Gheysarian, A. and Honarpisheh, M. (2021). Experimental and Numerical Investigation of Process Parameters on the Residual Stresses in the Al-Cu FGM Materials. Experimental Techniques, 45(5), pp. 601-612. DOI: 10.1007/s40799-021-00444-6.

[2] Shen, W., Chen, Y., Li, G., Lei, J., Chen, W. and Qiu, Y. (2023). Semi-empirical formulas on notch stress field and SIF of orthotropic V-shaped thin plate with initial crack under tensile-bending loads. Engineering Fracture Mechanics, 281, 109040. DOI: 10.1016/j.engfracmech.2022.109040.

[3] Kong, W., Dai, Y. and Liu, Y. (2022). Three-dimensional sharp V-notch stress intensity factor and strain energy rate density under creeping conditions. Engineering Fracture Mechanics, 272, 108700. DOI: 10.1016/ j.engfracmech.2022.108700.

[4] Gong, C., Niu, T.-Y., Gong, J.-G. and Xuan, F.-Z. (2021). A time-dependent stress and strain estimation method for notched components under displacement-controlled condition. Engineering Fracture Mechanics, 242, 107447. DOI: 10.1016/j.engfracmech.2020.107447.

[5] Wang, W., Yuan, H., Li, X. and Shi, P. (2019). Stress Concentration and Damage Factor Due to Central Elliptical Hole in Functionally Graded Panels Subjected to Uniform Tensile Traction. Materials, 12(3), 422. DOI: 10.3390/ma12030422.

[6] Kubair, D. V. and Bhanu-Chandar, B. (2008). Stress concentration factor due to a circular hole in functionally graded panels under uniaxial tension. International Journal of Mechanical Sciences, 50(4), pp. 732-742. DOI: 10.1016/j.ijmecsci.2007.11.009.

[7] Dave, J. M. and Sharma, D. S. (2018). Stress field around rectangular hole in functionally graded plate. International Journal of Mechanical Sciences, 136, pp. 360-370. DOI: 10.1016/j.ijmecsci.2017.12.010.

[8] Enab, T. A. (2014). Stress concentration analysis in functionally graded plates with elliptic holes under biaxial loadings. Ain Shams Engineering Journal, 5(3), pp. 839-850. DOI: 10.1016/j.asej.2014.03.002.

[9] Cárdenas-García, J. F., Shabana, Y. M. and Medina, R. A. (2006). Thermal loading and material property characterization of a functionally graded plate with a hole using an inverse problem methodology. Journal of Thermal Stresses, 29(1), pp. 1-20. DOI: 10.1080/014957390967929.

[10] Yang, Y., Cheng, Y. and Zhu, W. (2018). Stress concentration around a rectangular cuboid hole in a three-dimensional elastic body under tension loading. Archive of Applied Mechanics, 88(8), pp. 1229-1241. DOI: 10.1007/s00419-018-1369-7.

[11] Mohammadi, M., Dryden, J. R. and Jiang, L. (2011). Stress concentration around a hole in a radially inhomogeneous plate. International Journal of Solids and Structures, 48(3), pp. 483-491. DOI: 10.1016/j.ijsolstr.2010.10.013.

[12] Bansal, M., Singh, I. V., Mishra, B. K., Sharma, K. and Khan, I. A. (2017). A stochastic XFEM model for the tensile strength prediction of heterogeneous graphite based on microstructural observations. Journal of Nuclear Materials, 487, pp. 143-157. DOI: 10.1016/j.jnucmat.2016.12.045.
[13] Singh, I. V., Mishra, B. K., Bhattacharya, S. and Patil, R. U. (2012). The numerical simulation of fatigue crack growth using extended finite element method. International Journal of Fatigue, 36(1), pp. 109-119. DOI: 10.1016/ j.ijfatigue.2011.08.010.
[14] Xu, Y. and Yuan, H. (2009). On damage accumulations in the cyclic cohesive zone model for XFEM analysis of mixed-mode fatigue crack growth. Computational Materials Science, 46(3), pp. 579-585. DOI: 10.1016/ j.commatsci.2009.04.029.
[15] Asadpoure, A., Mohammadi, S. and Vafai, A. (2006). Crack analysis in orthotropic media using the extended finite element method. Thin-Walled Structures, 44(9), pp. 1031-1038. DOI: 10.1016/j.tws.2006.07.007.
[16] Khazal, H., Bayesteh, H., Mohammadi, S., Ghorashi, S. S. and Ahmed, A. (2016). An extended element free Galerkin method for fracture analysis of functionally graded materials. Mechanics of Advanced Materials and Structures,23(5), pp. 513-528. DOI: 10.1080/15376494.2014.98409 3.
[17] Ueda, S. (2001). Elastoplastic analysis of W-Cu functionally graded materials subjected to a thermal shock by micromechanical model. Journal of Thermal Stresses, 24(7), pp. 631-649. DOI: 10.1080/014957301300194 814.
[18] Lee, J.-M. and Toi, Y. (2002). Elasto-plastic damage analysis of functionally graded materials subjected to thermal shock and thermal cycle. JSME International Journal Series A Solid Mechanics and Material Engineering, 45(3), pp. 331-338. DOI: 10.1299/jsmea.45.331.
[19] Grujicic, M. and Zhang, Y. (1998). Determination of effective elastic properties of functionally graded materials using Voronoi cell finite element method. Materials Science and Engineering: A, 251(1), pp. 64-76. DOI: 10.1016/S0921-5093(98)00647-9.
[20] Egner, H., Juchno, M., Kula, M. and Skrzypek, J. (2007). Numerical analysis of FG and TBC systems based on thermo-elasto-plastic-damage model. Journal of Thermal Stresses, 30(9-10), pp. 977-1001. DOI: 10.1080 /01495730701499057.
[21] Tilbrook, M., Rutgers, L., Moon, R. J. and Hoffman, M. (2005). Fracture and fatigue crack propagation in graded composites. In Materials Science Forum. Trans Tech Publ. DOI: 10.4028/www.scientific.net/MSF.492-493.573
[22] Kim, J. H. and Paulino, G. H. (2005). Mixed-mode crack propagation in functionally graded materials. In Materials Science Forum. Trans Tech Publ, 492–493, pp. 409–14. DOI: 10.4028/www.scientific.net/msf.492-493.409.
[23] Barretta, R. and Marotti de Sciarra, F. (2013). A nonlocal model for carbon nanotubes under axial loads. Advances in Materials Science and Engineering. DOI: 10.1155/2013/360935.
[24] Barretta, R., Čanađija, M., Luciano, R. and de Sciarra, F. M. (2018). Stress-driven modeling of nonlocal thermoelastic behavior of nanobeams. International Journal of Engineering Science, 126, pp.53-67. DOI: 10 .1016 /j.ijengsci.2018.02.012.
[25] Zivelonghi, A. and You, J.-H. (2014). Mechanism of plastic damage and fracture of a particulate tungsten-reinforced copper composite: A microstructure-based finite element study. Computational Materials Science, 84, pp. 318-326. DOI: 10.1016/j.commatsci.2013.11.067.
[26] Gunes, R., Aydin, M., Apalak, M. K. and Reddy, J. N. (2011). The elasto-plastic impact analysis of functionally graded circular plates under low-velocities. Composite Structures, 93(2), pp. 860-869. DOI: 10.1016/ j.compstruct.2010.07.008.
[27] Huang, H., Chen, B. and Han, Q. (2014). Investigation on buckling behaviors of elastoplastic functionally graded cylindrical shells subjected to torsional loads. Composite Structures, 118, pp. 234-240. DOI: 10.1016/ j.compstruct.2014.07.025.
[28] Zhang, Y., Huang, H. and Han, Q. (2015). Buckling of elastoplastic functionally graded cylindrical shells under combined compression and pressure. Composites Part B: Engineering, 69, pp. 120-126. DOI: 10.1016/ j.compositesb.2014.09.024.
[29] Jrad, H., Mars, J., Wali, M. and Dammak, F. (2019). Geometrically nonlinear analysis of elastoplastic behavior of functionally graded shells. Engineering with Computers, 35(3), pp. 833-847. DOI: 10.1007/s00366-018-0633-3.
[30] Amirpour, M., Das, R. and Bickerton, S. (2017). An elasto-plastic damage model for functionally graded plates with in-plane material properties variation: Material model and numerical implementation. Composite Structures, 163, pp. 331-341. DOI: 10.1016/j.compstruct.2016.12.020.
[31] Feulvarch, E., Lacroix, R. and Deschanels, H. (2020). A 3D locking-free XFEM formulation for the von Mises elasto-plastic analysis of cracks. Computer Methods in Applied Mechanics and Engineering, 361, 112805. DOI: 10.1016/j.cma.2019.112805.
[32] Jin, Z.-H., Paulino, G. H. and Dodds, R. H. (2003). Cohesive fracture modeling of elastic–plastic crack growth in functionally graded materials. Engineering Fracture Mechanics, 70(14), pp. 1885-1912.

DOI: 10.1016/S0013 -7944(03)00130-9.
[33] Khatri, K. and Lal, A. (2018). Stochastic XFEM fracture and crack propagation behaviour of an isotropic plate with hole emanating radial cracks subjected to various in-plane loadings. Mechanics of Advanced Materials and Structures, 25(9), pp. 732-755. DOI: 10.1080/15376494.2017.1308599.
[34] Khatri, K. and Lal, A. (2018). Stochastic XFEM based fracture behaviour and crack growth analysis of a plate with a hole emanating cracks under biaxial loading. Theoretical and Applied Fracture Mechanics, 96, pp. 1-22. DOI: 10.1016/j.tafmec.2018.03.009.
[35] Hirshikesh, S. Natarajan, R. K., Annabattula, R. and Martínez-Pañeda, E. (2019). Phase field modelling of crack propagation in functionally graded materials. Composites Part B: Engineering, 169, pp. 239-248. DOI: 10.1016/j.compositesb.2019.04.003.
[36] Batra, R. C. and Love, B. M. (2005). Crack propagation due to brittle and ductile failures in microporous thermoelastoviscoplastic functionally graded materials. Engineering Fracture Mechanics, 72(12), pp. 1954-1979. DOI: 10.1016/j.engfracmech.2004.11.010.
[37] Ritchie, R. O., Knott, J. F. and Rice, J. R. (1973). On the relationship between critical tensile stress and fracture toughness in mild steel. Journal of the Mechanics and Physics of Solids, 21(6), pp. 395-410. DOI: 10.1016/ 0022-5096(73)90008-2.
[38] Erdogan, F. and Sih, G. C. (1963). On the Crack Extension in Plates Under Plane Loading and Transverse Shear. Journal of Basic Engineering, 85(4), pp. 519-525. DOI: 10.1115/1.3656897.
[39] Hussain, M., Pu, S. and Underwood, J. (1974). Strain energy release rate for a crack under combined mode I and mode. Fracture analysis, 560(1).
[40] Bouchikhi, A. S., Lousdad, A., Yassine, K., Bouida, N. E., Gouasmi, S. and Megueni, A. (2019). Finite Element Analysis of Interactions of between two cracks in FGM notched Plate under Mechanical Loading. Frattura ed Integrità Strutturale, 13(48), pp. 174-192. DOI: 10.3221/IGF-ESIS.48.20.
[41] Mars, J., Said, L. B., Wali, M. and Dammak, F. (2018). Elasto-Plastic Modeling of Low-Velocity Impact on Functionally Graded Circular Plates. International Journal of Applied Mechanics, 10(04), 1850038. DOI: 10.1142/s1758825118500382.
[42] Martínez-Pañeda, E. and Gallego, R. (2015). Numerical analysis of quasi-static fracture in functionally graded materials. International Journal of Mechanics and Materials in Design, 11(4), pp. 405-424. DOI: 10.1007/s10999-014-9265-y.
[43] Burlayenko, V. N., Altenbach, H., Sadowski, T. and Dimitrova, S. D. (2016). Computational simulations of thermal shock cracking by the virtual crack closure technique in a functionally graded plate. Computational Materials Science, 116, pp. 11-21. DOI: 10.1016/j.commatsci.2015.08.038.
[44] Gunes, R., Aydin, M., Apalak, M. K. and Reddy, J. N. (2014). Experimental and numerical investigations of low velocity impact on functionally graded circular plates. Composites Part B: Engineering, 59, pp. 21-32. DOI: 10.1016/j.compositesb.2013.11.022.
[45] Kim, J.-H. and Paulino, G. H. (2002). Isoparametric Graded Finite Elements for Nonhomogeneous Isotropic and Orthotropic Materials. Journal of Applied Mechanics, 69(4), pp. 502-514. DOI: 10.1115/1.1467094.
[46] Williamson, R. L., Rabin, B. H. and Drake, J. T. (1993). Finite element analysis of thermal residual stresses at graded ceramic-metal interfaces. Part I. Model description and geometrical effects. Journal of Applied Physics, 74(2), pp. 1310-1320. DOI: 10.1063/1.354910.
[47] Houari, A., Mokhtari, M., Bouchikhi, A. S., Polat, A. and Madani, K. (2021). Using finite element analysis to predict the damage in FGM-3D notched plate under tensile load; Different geometric concept. Engineering Structures, 237, 112160. DOI: 10.1016/j.engstruct.2021.112160.
[48] Kumar, S., Shedbale, A. S., Singh, I. V. and Mishra, B. K. (2015). Elasto-plastic fatigue crack growth analysis of plane problems in the presence of flaws using XFEM. Frontiers of Structural and Civil Engineering, 9(4), pp. 420-440. DOI: 10.1007/s11709-015-0305-y.
[49] Malavika, V. A., Asraff, A. K., Kumar, M. and Sofi, A. (2021). Fracture analysis of plates and shells using FEM and XFEM. Innovative Infrastructure Solutions, 6(1), 43. DOI: 10.1007/s41062-020-00439-z.
[50] Sukumar, N. and Prévost, J. H. (2003). Modeling quasi-static crack growth with the extended finite element method Part I: Computer implementation. International Journal of Solids and Structures, 40(26), pp. 7513-7537. DOI: 10.1016/j.ijsolstr.2003.08.002.
[51] Hillerborg, A., Modéer, M. and Petersson, P. E. (1976). Analysis of crack formation and crack growth in concrete by means of fracture mechanics and finite elements. Cement and Concrete Research, 6(6), pp. 773-781. DOI: 10.1016/0008-8846(76)90007-7.

[52] Jin, Z. H. and Batra, R. C. (1996). Some basic fracture mechanics concepts in functionally graded materials. Journal of the Mechanics and Physics of Solids, 44(8), pp. 1221-1235. DOI: 10.1016/0022-5096(96)00041-5.
[53] Surya, M. S. and Prasanthi, G. (2019). Manufacturing and mechanical behavior of (Al/SiC) functionally graded material using powder metallurgy technique. Int J Innov Technol Expl Eng (IJITEE), 8(9), pp. 1835-1839. DOI: 10.35940/ijitee.I8215.078919

APPENDIX: PROGRAM FOR FGM

```
**********************************************************************
** USDFLD FOR FGM
** HOUARI AMIN ** University of Boumerdes
** E-mail: a.houari@univ-boumerdes.dz
** Predicting damage in notched functionally graded materials plates
** Through extended finite element method based on computational simulations (2024)
**********************************************************************
      SUBROUTINE USDFLD(FIELD,STATEV,PNEWDT,DIRECT,T,CELENT,
     1 TIME,DTIME,FGM,AMIN,NFIELD,NSTATV,NOEL,NPT,LAYER,
     2 KSPT,KSTEP,KINC,NDI,NSHR,COORD,JMAC,JMATYP,MATLAYO,LACCFLA)
C
      INCLUDE 'ABA_PARAM.INC'
C
      CHARACTER*80 CMNAME,ORNAME
      CHARACTER*3  FLGRAY(15)
      DIMENSION FIELD(NFIELD),STATEV(NSTATV),DIRECT(3,3),
     1 T(3,3),TIME(2)
      DIMENSION ARRAY(15),JARRAY(15),JMAC(*),JMATYP(*),COORD(*)
C     DIMENSION INTV(1),REALV(1)
        Z=COORD(3) ** Z: defines in our program the coordinate of the declared area.
C     READ X COORDONE
        FIELD(1) = Z
      RETURN
      END
```